

Experimental determination of the phase equilibria in the Mg–Zn–Sr ternary system

Jian Wang¹ · Yi-Nan Zhang² · Pierre Hudon³ · Patrice Chartrand¹ · In-Ho Jung³ · Mamoun Medraj^{2,4}

Received: 10 March 2015 / Accepted: 1 August 2015 / Published online: 8 August 2015
© Springer Science+Business Media New York 2015

Abstract Phase equilibria in the Mg–Zn–Sr ternary system, in the composition range 0–35 at% Sr at 300 °C, were investigated using two diffusion couples and 23 alloy samples. Scanning electron microscopy equipped with an energy-dispersive spectroscope and electron probe microanalysis were employed to analyze the constituted phases and their compositions in diffusion couples and alloy samples. X-ray diffraction (XRD) was used to analyze the crystal structure of the constituted phases in selected samples. Four new ternary compounds, $\text{Mg}_{11-y}\text{Zn}_y\text{Sr}$ ($4.7 < y < 9$), $\text{Mg}_{44}\text{Zn}_{21}\text{Sr}_{35}$, $\text{Mg}_{20}\text{Zn}_{62}\text{Sr}_{18}$, and $\text{Mg}_{55}\text{Zn}_{43}\text{Sr}_2$ were discovered in the Mg–Zn–Sr ternary system at 300 °C. In total, sixteen three-phase equilibria regions were determined in the present work. The isothermal phase diagram of the Mg–Zn–Sr ternary system, in the composition range 0–35 at% Sr, was constructed at 300 °C.

Introduction

Mg-based alloys, with low density and high strength/weight ratios and near complete recycling potential, are widely used in the automotive and aeronautic industries [1]. The Mg–Zn series alloys, as the hardenable alloys, have been developed as structural materials [2] for several decades. A very good age-hardening effect can be achieved with the dissolution of Zn and the precipitates of secondary phase in the hcp (Mg) matrix with the heat treatment [3]. Unfortunately, the Mg–Zn-based alloys have the same problem as the Mg–Al series (but not the AE series), that is, poor mechanical properties at elevated temperatures which restrict their applications [4]. Recently, strontium has drawn much attention [5–9] as an important additive of Mg-based alloys for improving relatively high-temperature mechanical properties. According to Baril et al. [8], the micro-alloying of strontium in Mg-based alloys (e.g., Mg–Zn and Mg–Al series) leads to superior creep performance and excellent high-temperature mechanical properties. Moreover, Hirai et al. [9] reported that by adding Sr, high strength, and improved creep resistance could be obtained for the cast AZ91 alloys. Since Sr acts as an important micro-alloying element for Mg–Zn-based alloys, a comprehensive understanding of the phase equilibria in the Mg–Zn–Sr ternary system, especially in the Mg-rich region, is of primary importance for Mg-based alloys development.

The phase diagrams of the three binary sub-systems Mg–Zn [10–13], Mg–Sr [14], and Zn–Sr [15] of the Mg–Zn–Sr ternary system have been satisfactorily investigated using experimental and thermodynamic modeling methods. The final accepted version of each binary phase diagram is shown in Fig. 1. The phase diagram of the Mg–Zn binary system includes five intermetallic compounds, $\text{Mg}_2\text{Zn}_{11}$,

✉ Jian Wang
jian.wang@polymtl.ca

¹ Center for Research in Computational Thermochemistry (CRCT), Department of Chemical Engineering, École Polytechnique, Montréal, QC H3C 3A7, Canada

² Department of Mechanical Engineering, Concordia University, 1455 De Maisonneuve Blvd. West, Montreal, QC H3G 1M8, Canada

³ Department of Mining and Materials Engineering, McGill University, 3610 University Street, Montreal, QC H3A 0C5, Canada

⁴ Department of Mechanical and Materials Engineering, Masdar Institute, P.O. Box 54224, Masdar City, Abu Dhabi, UAE

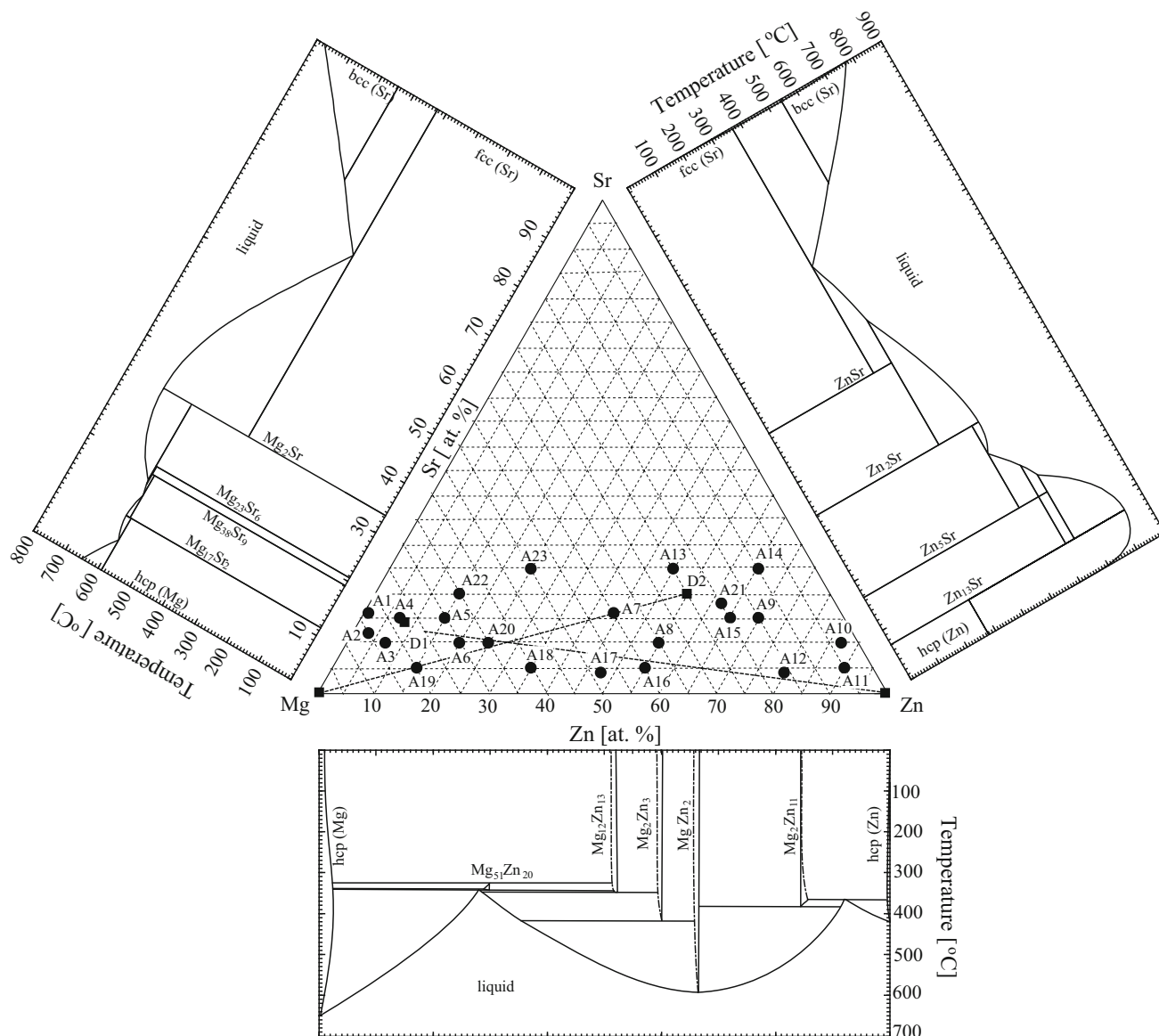


Fig. 1 Phase diagrams of the bounding binary sub-systems of the Mg–Zn–Sr ternary system along with the compositions of the samples used in the present work

MgZn₂, Mg₂Zn₃, Mg₁₂Zn₁₃, and Mg₅₁Zn₂₀, and two terminal solid solutions, hcp (Mg) and hcp (Zn). It is worth noting that Mg₅₁Zn₂₀, with minimum solid solubility, is stable only between 325 and 342 °C [16]. The phase diagram of the Mg–Sr binary system contains seven solid phases: hcp (Mg), fcc (Sr), bcc (Sr), Mg₁₇Sr₂, Mg₃₈Sr₉, Mg₂₃Sr₆, and Mg₂Sr. Four stoichiometric compounds, ZnSr, Zn₂Sr, Zn₅Sr, and Zn₁₃Sr, plus three terminal solid solutions, hcp (Zn), fcc (Sr), and bcc (Sr) with limited solid solubility, constitute the phase diagram of the Zn–Sr binary system. Aljarrah et al. [17] extrapolated the Mg–Zn–Sr ternary system using the CALPHAD method [18] based on the thermodynamic parameters of the three binary sub-

systems. To date, no experimental data, except the study on the crystal structure and solid solubility limits of compound Mg_{15–x}Zn_xSr₃ submitted for publication by our group [19], have been reported on the phase equilibria of the Mg–Zn–Sr ternary system. All the phases of the Mg–Zn–Sr ternary system and their crystallographic information are summarized in Table 1.

In order to obtain a comprehensive understanding of the phase equilibria in the Mg–Zn–Sr ternary system for Mg-based alloys development purpose, the isothermal section of the Mg–Zn–Sr ternary system, in the Mg–Zn rich composition region (0–35 at% Sr) at 300 °C, was studied using diffusion couples and equilibrated key samples. The

Table 1 Crystallographic information on the solid phases in the Mg–Zn–Sr ternary system

System	Phase	Pearson symbol	Strukturbericht designation	Space group	Prototype
Mg–Zn	hcp (Mg)	<i>hP2</i>	A3	$P6_3/mmc$	Mg
	hcp (Zn)	<i>hP2</i>	A3	$P6_3/mmc$	Mg
	Mg ₁₂ Zn ₁₃	–	–	–	–
	Mg ₂ Zn ₃	<i>mC110</i>	–	$B2/m$	–
	MgZn ₂	<i>hP12</i>	C14	$P6_3/mmc$	MgZn ₂
	Mg ₂ Zn ₁₁	<i>cP39</i>	D8 _c	$Pm\bar{3}$	Mg ₂ Zn ₁₁
	Mg ₅₁ Zn ₂₀	<i>oI142</i>	D7 _b	<i>Immm</i>	Ta ₃ B ₄
Mg–Sr	hcp (Mg)	<i>hP2</i>	A3	$P6_3/mmc$	Mg
	bcc (Sr)	<i>cI2</i>	A2	$Im\bar{3}m$	W
	fcc (Sr)	<i>cF4</i>	A1	$Fm\bar{3}m$	Cu
	Mg ₁₇ Sr ₂	<i>hp38</i>	–	$P6_3/mmc$	Ni ₁₇ Th ₂
	Mg ₃₈ Sr ₉	<i>hP94</i>	–	$P6_3/mmc$	Mg ₃₈ Sr ₉
	Mg ₂₃ Sr ₆	<i>cF116</i>	D8 _a	$Fm\bar{3}m$	Mn ₂₃ Th ₆
	Mg ₂ Sr	<i>hP12</i>	C14	$P6_3/mmc$	MgZn ₂
Zn–Sr	bcc (Sr)	<i>cI2</i>	A2	$Im\bar{3}m$	W
	fcc (Sr)	<i>cF4</i>	A1	$Fm\bar{3}m$	Cu
	hcp (Zn)	<i>hP2</i>	A3	$P6_3/mmc$	Mg
	ZnSr	<i>oP8</i>	B27	<i>Pnma</i>	FeB
	Zn ₂ Sr	<i>oI12</i>	–	<i>Imma</i>	CeCu ₂
	Zn ₅ Sr (LT)	<i>oP24</i>	–	<i>Pnma</i>	Zn ₅ Sr
	Zn ₅ Sr (HT)	<i>hP6</i>	D2 _d	$P6/mmm$	CaCu ₅
	Zn ₁₃ Sr	<i>cF112</i>	D2 ₃	$Fm\bar{3}c$	NaN ₁₃

selection of diffusion couples and key samples was based on the extrapolated results with the three binary sub-systems. Moreover, the phase equilibria reported previously in the Mg–Zn–Ca ternary system [20] were also taken as a reference due to the similar chemical properties of Ca and Sr. The samples and diffusion couple (Mg–Mg₂₅Zn₅₅Sr₂₀) discussed in our previous work [19] were reinvestigated for the phase equilibria measurements of the Mg–Zn–Sr ternary system. The target temperature of 300 °C was chosen because it corresponds to the temperature at which heat treatments are usually performed on Mg alloys. The present work is part of a wider thermodynamic database development project of Mg–X (X: Ag, Ca, In, Li, Na, Sn, Sr, and Zn)-based alloys for automotive applications [19–29].

Experimental procedure

Two solid-state diffusion couples and 32 ternary alloy samples of the Mg–Zn–Sr system were prepared using pure Mg (99.8 wt%), Zn (99.5 wt%), and Sr (99 wt%) obtained from Alfa Aesar. The nominal compositions of the end-members of the diffusion couples and other alloy samples are given in Tables 2 and 3, respectively, and shown Fig. 1. The Sr pieces were stored in oil after weighing due to the high reactivity of Sr with oxygen. Before melting,

each Sr piece was washed carefully with 99 wt% ethanol to remove the oil. In order to minimize the interaction of the samples with the crucibles, cubic-shaped crucibles were made using Ta foil (99.5 wt% purity, 0.15 mm thickness). All samples were re-melted at least 3 times in the induction furnace under argon in order to obtain a homogeneous alloy. To prepare solid-state diffusion couples, the contacting surfaces of the alloy pieces were ground with 1200 grit SiC paper and polished using a 1 μm oil-based diamond suspension with 99 % pure ethanol as lubricant. The end-members were gently pressed and clamped with a steel ring. Diffusion couples and alloy samples were then sealed into quartz capsules under argon and equilibrated at 300 °C for 21 and 35 days, respectively. Quenching was carried out in water without breaking the quartz tube to avoid any reaction of the samples with water.

Phase relationships and constitution of the alloy samples were analyzed using electron probe micro-analysis (EPMA) with wavelength dispersive X-ray spectrometry (WDS) and scanning electron microscopy (SEM) equipped with an energy-dispersive spectroscope (EDS). An accelerating voltage of 15 kV was used for the EPMA/EDS analysis with a 20 nA beam current, a spot size of 2 μm and counting times of 20 s on peaks and 10 s on backgrounds. Raw data were reduced with the phi-rho-Z (PRZ) correction using pure Mg, Zn metal, and SrO standards.

Table 2 Equilibrium compositions obtained from the Mg–Zn–Sr diffusion couples at 300°C

Diffusion couples	Phase equilibria Phase 1/Phase 2/Phase 3	Composition determined by EDS (at%)								
		Phase 1			Phase 2			Phase 3		
		Mg	Zn	Sr	Mg	Zn	Sr	Mg	Zn	Sr
D1 (Zn–Mg ₇₅ Zn _{12.5} Sr _{12.5})	Mg _{15–x} Zn _x Sr ₃ /Mg ₁₇ Sr ₂ /—	69.3	14.1	16.7	79.5	10.4	10.1	–	–	–
	Mg _{15–x} Zn _x Sr ₃ /Mg ₁₇ Sr ₂ /—	69.0	14.5	16.5	78.7	10.7	10.6	–	–	–
	Mg _{15–x} Zn _x Sr ₃ /Mg ₁₇ Sr ₂ /—	68.2	15.3	16.5	78.4	11.3	10.3	–	–	–
	Mg _{15–x} Zn _x Sr ₃ /Mg _{11–y} Zn _y Sr—	54.7	29.5	15.8	48.7	42.1	9.2	–	–	–
	Mg _{15–x} Zn _x Sr ₃ /Mg _{11–y} Zn _y Sr—	54.2	30.3	15.6	47.6	43.4	9.0	–	–	–
	Mg _{11–y} Zn _y Sr/MgZn ₂ /—	32.2	67.6	17.2	10.4	80.4	9.2	–	–	–
	Mg _{11–y} Zn _y Sr/MgZn ₂ /—	24.6	66.1	9.3	33.4	66.2	0.4	–	–	–
	Mg _{11–y} Zn _y Sr/MgZn ₂ /—	18.2	73.0	8.8	32.8	66.6	0.6	–	–	–
D2 (Zn–Mg ₅₅ Zn ₁₀ Ag ₃₅)	Mg _{15–x} Zn _x Sr ₃ /Zn ₂ Sr/—	30.2	52.0	17.8	1.3	65.2	33.5	–	–	–
	Mg _{15–x} Zn _x Sr ₃ /Mg _{11–y} Zn _y Sr/—	54.4	29.3	16.3	50.6	40.6	8.8	–	–	–
	Mg _{11–y} Zn _y Sr/Mg ₁₇ Sr ₂ /—	5.3	37.8	8.9	71.4	19.1	9.5	–	–	–
	hcp (Mg)/Mg ₁₇ Sr ₂ /—	98.4	1.3	0.3	73.5	18.2	8.3	–	–	–
	Mg _{15–x} Zn _x Sr ₃ /Mg _{11–y} Zn _y Sr/Mg ₁₇ Sr ₂	56.2	27.9	15.9	49.7	41.0	9.3	70.1	19.9	10.0

Phase relationships and constitutions of the diffusion couples were determined using SEM/EDS. An accelerating voltage of 20 kV was used with a spot size of 3 μm and counting times of 50 s. Five points in different areas of each target phase were measured using EPMA/EDS to obtain an average value of the phase composition.

Crystal structures of the phases present in the annealed samples were identified by X-ray diffraction (XRD). XRD patterns were obtained with a PAN analytical X’pert Pro powder X-ray diffractometer using CuKα radiation at 45 kV and 40 mA. The patterns were acquired from 20–120° (2θ) with a 0.02 step size. The collected patterns were analyzed with the X’Pert HighScore plus Rietveld analysis software in combination with the Pearson’s crystal database [30]. Si was used as an internal calibration standard to enable correcting the zero shift and specimen surface displacement, which are the most serious systematic errors in X-ray powder diffraction patterns.

Results and discussion

Diffusion couples results

In order to obtain general information on the equilibrium phase relationships in the Mg–Zn–Sr ternary system, two diffusion couples, D1 (Zn–Mg₇₅Zn_{12.5}Sr_{12.5}) and D2 (Mg–Mg₂₅Zn₅₅Sr₂₀), as shown in Fig. 1, were prepared and investigated.

Back-scattered electron (BSE) images obtained by SEM of the diffusion couple D1, with gradually increased

magnification of the area of interest, are shown in Fig. 2. During the heat treatment, extensive inter-diffusion of Mg, Zn, and Sr took place, allowing various equilibrated phases to form. As shown in Fig. 2a, several diffusion layers were formed in the diffusion couple D1 after the heat treatment. The new compound designated as Mg_{15–x}Zn_xSr₃ (with detailed crystal structure information given in Ref. [19]), in equilibrium with the Mg₁₇Sr₂ phase, was also observed in the end-member alloy Mg₇₅Zn_{12.5}Sr_{12.5} (at%), as shown in Fig. 2b. The equilibrium phase compositions of Mg_{15–x}Zn_xSr₃ and Mg₁₇Sr₂ in the diffusion couple D1, obtained using EDS, are listed in Table 2. In the diffusion couple D1, a second new ternary compound (Mg_{11–y}Zn_ySr), designated as IM1, IM3 and IM5 in our previous work [19], was observed as shown in Fig. 2c–e. According to the EDS analysis of the diffusion couple D1, the solid solubility of this compound ranges from about 42–81 at% Zn with a constant value of about 9 at% Sr. This compound was thus designated as IM1 (Mg_{11–y}Zn_ySr, 4.7 < y < 9) in the present work. The element compositions of Mg_{11–y}Zn_ySr and its equilibrated phases, obtained using EDS, are listed in Table 2. Taking advantage of the local equilibrium at the interfaces formed between the phases, the sequence of the phases formed and the diffusion path in the diffusion couple D1 could be deemed to be Mg_{15–x}Zn_xSr₃ + Mg₁₇Sr₂ ↔ Mg_{11–y}Zn_ySr + MgZn₂ ↔ Zn₁₃Sr ↔ Zn (hcp). The diffusion path of the diffusion couple D1 is shown in Fig. 3. Note that the diffusion interface of hcp (Zn) and Zn₁₃Sr was lost due to inevitable cracks which occurred during the quenching and polishing processes.

Table 3 Equilibrium compositions obtained from key samples in the Mg–Zn–Sr ternary system at 300 °C

Alloy no.	Alloy nominal composition (at%)	Phase equilibria Phase 1/Phase 2/Phase 3	Measured equilibrium phase compositions determined by EPMA (at%)								
			Phase 1			Phase 2			Phase 3		
			Mg	Zn	Sr	Mg	Zn	Sr	Mg	Zn	Sr
A1*	Mg ₈₃ Zn ₁ Sr ₁₆	Mg _{15-x} Zn _x Sr ₃ /Mg ₁₇ Sr ₂ /Mg ₃₈ Sr ₉	81.6	1.3	17.1	88.1	0.6	11.3	79.4	0.6	20.0
A2	Mg ₈₅ Zn ₃ Sr ₁₂	Mg _{15-x} Zn _x Sr ₃ /Mg ₁₇ Sr ₂	81.4	3.2	15.4	88.4	1.3	10.3	–	–	–
A3	Mg ₈₃ Zn ₇ Sr ₁₀	Mg _{15-x} Zn _x Sr ₃ /Mg ₁₇ Sr ₂	77.0	7.5	15.5	86.1	3.7	10.2	–	–	–
A4	Mg ₇₈ Zn ₇ Sr ₁₅	Mg _{15-x} Zn _x Sr ₃ /Mg ₁₇ Sr ₂	73.2	11.9	14.9	83.6	6.4	10.0	–	–	–
A5	Mg ₇₀ Zn ₁₅ Sr ₁₅	Mg _{15-x} Zn _x Sr ₃ /Mg ₂₃ Sr ₆	69.0	14.7	16.3	69.0	10.5	20.5	–	–	–
A6	Mg ₇₀ Zn ₂₀ Sr ₁₀	Mg _{15-x} Zn _x Sr ₃ /Mg ₁₇ Sr ₂	60.0	24.8	15.2	73.2	17.1	9.7	–	–	–
A7	Mg ₄₀ Zn ₄₄ Sr ₁₆	Mg _{15-x} Zn _x Sr ₃ /Mg ₂ Sr/Mg ₄₄ Zn ₂₁ Sr ₃₅	34.6	48.3	16.1	64.7	2.2	33.1	43.9	22.5	33.6
A8	Mg ₃₅ Zn ₅₅ Sr ₁₀	Mg _{15-x} Zn _x Sr ₃ /Mg _{11-y} Zn _y Sr	33.8	49.5	16.7	36.3	54.8	8.9	–	–	–
A9	Mg ₁₅ Zn ₇₀ Sr ₁₅	Mg _{11-y} Zn _y Sr/Zn ₅ Sr/Mg ₂₀ Zn ₆₂ Sr ₁₈	9.8	81.2	9.0	2.6	80.5	16.9	19.1	63.3	17.6
A10	Mg ₃ Zn ₈₇ Sr ₁₀	Zn ₅ Sr/Zn ₁₃ Sr/Mg _{11-y} Zn _y Sr	0.04	82.6	17.4	0.7	91.7	7.6	6.6	84.2	9.2
A11	Mg ₅ Zn ₉₀ Sr ₅	Mg ₂ Zn ₁₁ /Zn ₁₃ Sr/MgZn ₂	15.3	84.5	0.2	0.2	92.7	7.1	32.6	67.1	0.3
A12	Mg ₁₆ Zn ₈₀ Sr ₄	MgZn ₂ /Zn ₁₃ Sr/Mg _{11-y} Zn _y Sr	33.5	66.2	0.3	1.0	92.0	7.0	8.1	83.7	8.2
A13*	Mg ₂₅ Zn ₅₀ Sr ₂₅	Mg _{15-x} Zn _x Sr ₃ /Mg ₄₄ Zn ₂₁ Sr ₃₅ /Zn ₂ Sr	33.5	49.9	16.6	43.4	21.6	35.0	1.8	63.1	35.1
A14	Mg ₁₀ Zn ₆₅ Sr ₂₅	Zn ₂ Sr/Zn ₅ Sr/Mg ₂₀ Zn ₆₂ Sr ₁₈	0.6	65.3	34.1	2.1	80.5	17.4	18.7	63.2	18.1
A15*	Mg ₂₀ Zn ₆₅ Sr ₁₅	Mg _{15-x} Zn _x Sr ₃ /Mg _{11-y} Sr _y Zn/Mg ₂₀ Zn ₆₂ Sr ₁₈	24.9	58.8	16.3	11.8	79.6	8.6	20.4	61.8	17.8
A16	Mg ₄₀ Zn ₅₅ Sr ₅	Mg _{11-y} Zn _y Sr/Mg ₂ Zn ₃ /Mg ₁₂ Zn ₁₃	35.8	55.5	8.7	40.3	58.5	1.2	48.4	50.3	1.3
A17	Mg ₄₉ Zn ₄₇ Sr ₄	Mg _{11-y} Zn _y Sr/Mg ₅₅ Zn ₄₃ Sr ₂ /Mg ₁₂ Zn ₁₃	45.0	46.9	8.1	54.5	44.0	1.5	48.6	50.6	0.8
A18	Mg ₆₀ Zn ₃₅ Sr ₅	Mg _{11-y} Zn _y Sr/Mg ₅₅ Zn ₄₃ Sr ₂ /hcp	47.5	45.0	7.5	55.5	42.9	1.6	96.5	3.2	0.3
A19	Mg ₈₀ Zn ₁₅ Sr ₅	Mg _{11-y} Zn _y Sr/Mg ₁₇ Sr ₂ /hcp	48.1	44.5	7.4	72.4	18.1	9.5	98.5	1.3	0.2
A20	Mg ₆₅ Zn ₂₅ Sr ₁₀	Mg _{11-y} Zn _y Sr/Mg _{15-x} Zn _x Sr ₃ /Mg ₁₇ Sr ₂	49.0	42.0	9.0	58.1	26.4	15.5	69.1	20.2	10.7
A21*	Mg ₂₀ Zn ₆₂ Sr ₁₈	Zn ₂ Sr/Mg ₂₀ Zn ₆₂ Sr ₁₈ /Mg _{15-x} Zn _x Sr ₃	1.6	65.5	32.9	19.6	62.5	17.9	25.9	57.8	16.3
A22	Mg ₆₅ Zn ₁₅ Sr ₂₀	Mg _{15-x} Zn _x Sr ₃ /Mg ₂₃ Sr ₆ /Mg ₂ Sr	59.9	23.6	16.5	67.6	12.4	20.0	65.2	1.5	33.3
A23*	Mg ₅₀ Zn ₂₅ Sr ₂₅	Mg _{15-x} Zn _x Sr ₃ /Mg ₄₄ Zn ₂₁ Sr ₃₅ /Mg ₂ Sr	35.3	48.6	16.1	44.2	21.1	34.7	64.3	2.5	33.3

* The values were taken from EDS and corrected by EPMA with standards; The phase constitution and composition of A1–A8 and A15 was reinvestigated basing results from Ref. [19]

The diffusion couple D2 has been investigated to analyze the solid solubility of the new compound Mg₁₁Zn₄Sr₃ reported in our previous work [19]. In this section, the phase equilibrium information obtained from the diffusion couple D2 was reinvestigated and further discussed. BSE images of the diffusion couple D2 are shown in the Fig. 4. Four diffusion layers, viz., Mg_{15-x}Zn_xSr₃, Mg_{11-y}Zn_ySr, Mg₁₇Sr₂, and hcp (Mg), were observed as shown in Fig. 4a. The two-phase equilibrated microstructure Zn₂Sr + Mg_{15-x}Zn_xSr₃ was observed in the end-member of Mg₂₅Zn₅₅Sr₂₀ alloy as shown in Fig. 4b. The EDS analytical results on the constituted phase compositions are listed in Table 2. The solid solubility of Mg in Zn₂Sr was measured to be about 1.3 at%. However, according to the composition value of 17.8 at% Sr obtained in the constituted phase of Mg_{15-x}Zn_xSr₃, the two phases Zn₂Sr and Mg_{15-x}Zn_xSr₃ in the end-member of Mg₂₅Zn₅₅Sr₂₀ alloy need more time to reach complete equilibrium. The phase Mg_{11-y}Zn_ySr, found in the diffusion couple D1, was also

observed in the diffusion couple D2 in the three-phase equilibrated microstructure Mg_{15-x}Zn_xSr₃ + Mg_{11-y}Zn_ySr + Mg₁₇Sr₂ (see Fig. 4a, c). The equilibrium composition of each phase of Mg_{15-x}Zn_xSr₃, Mg_{11-y}Zn_ySr, and Mg₁₇Sr₂, in the three-phase assemblage Mg_{15-x}Zn_xSr₃ + Mg_{11-y}Zn_ySr + Mg₁₇Sr₂, was measured at the position where all the three phases existed (marked as triangles in Fig. 4c). Average values were obtained with more than 5 different measurement positions, which were summarized in Table 2.

The sequence of the diffusion paths in the diffusion couple D2 was determined as follows Mg_{15-x}Zn_xSr₃ ↔ Mg_{11-y}Zn_ySr + Mg_{15-x}Zn_xSr₃ + Mg₁₇Sr₂ ↔ Mg₁₇Sr₂ + Mg (hcp) ↔ Mg (hcp) as shown in Figs. 3 and 4. The EDS line scan was used to determine the composition profile of phases formed as shown in Fig. 4d. According to the acquired line-scan results, the solid solubility limit of Zn in Mg_{15-x}Zn_xSr₃ was found to be about 29–37 at% with substitution of Mg at a constant Sr content of about 16.7

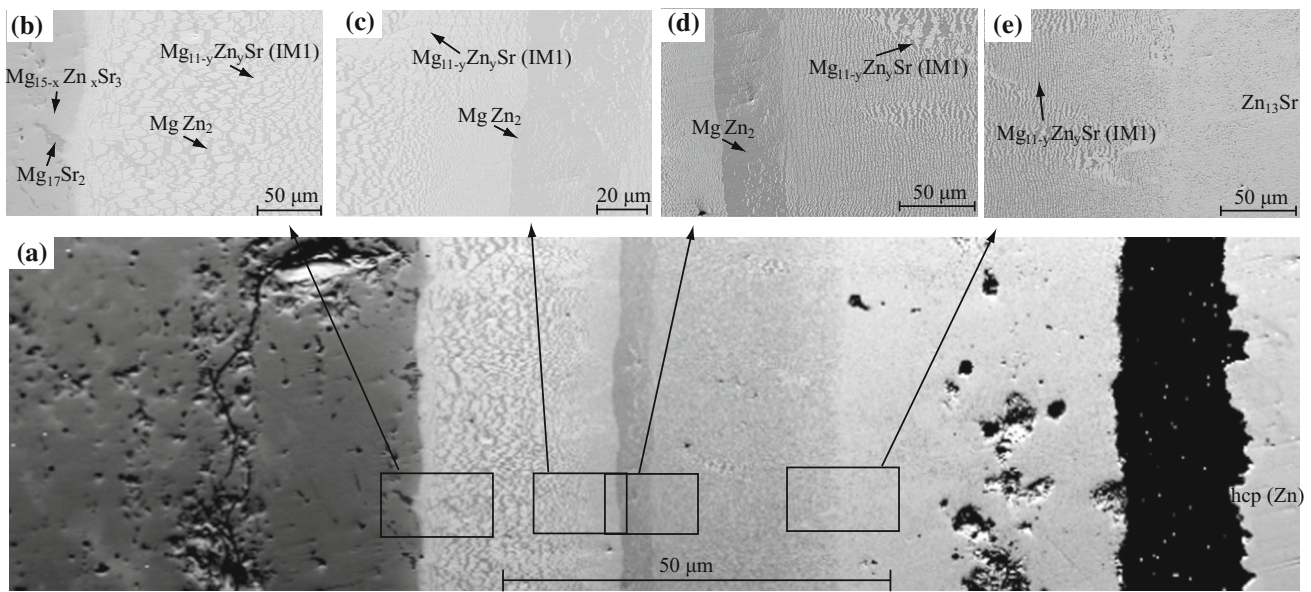


Fig. 2 a BSE image of diffusion couple D1 (Zn–Mg₇₅Zn_{12.5}Sr_{12.5}); **b–e** enlarged BSE images of boxed areas from the lower image of D1

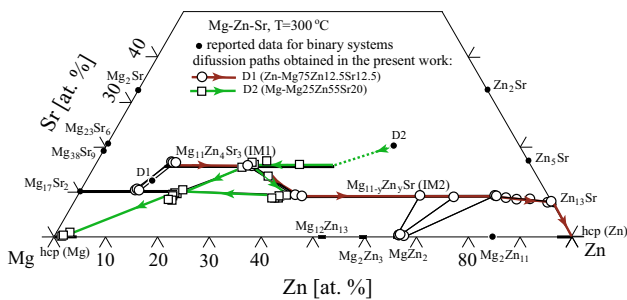


Fig. 3 Isothermal section of the Mg–Zn–Sr ternary at 300 °C with experimental data obtained from diffusion couples

at%. Equilibrium compositions of the constituted phases, obtained from the diffusion couple D2 using EDS, are summarized in Table 2.

According to the analytical results from the two diffusion couples D1 and D2, a new compound IM1 (Mg_{11–y}Zn_ySr, 4.7 < y < 9) was observed in the Mg–Zn–Sr ternary system at 300 °C. More accurate solubilities were further confirmed and measured using the following alloy samples.

Alloy samples results

Based on the phase equilibria relationships obtained from diffusion couples D1 and D2, 23 samples (A1–A23) were selected and prepared in order to confirm the phase relationships, and to construct an isothermal section of the Mg–Zn–Sr ternary system at 300 °C.

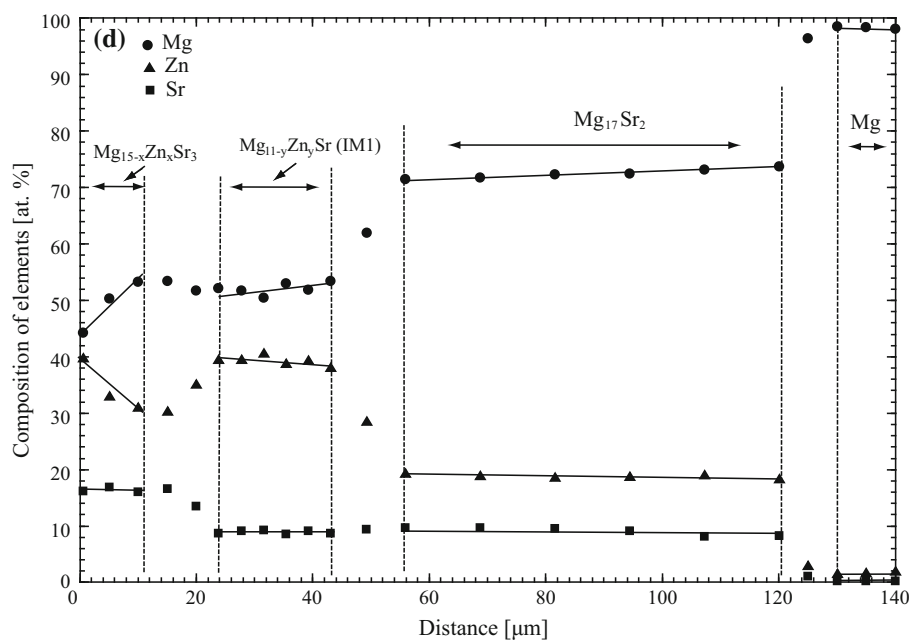
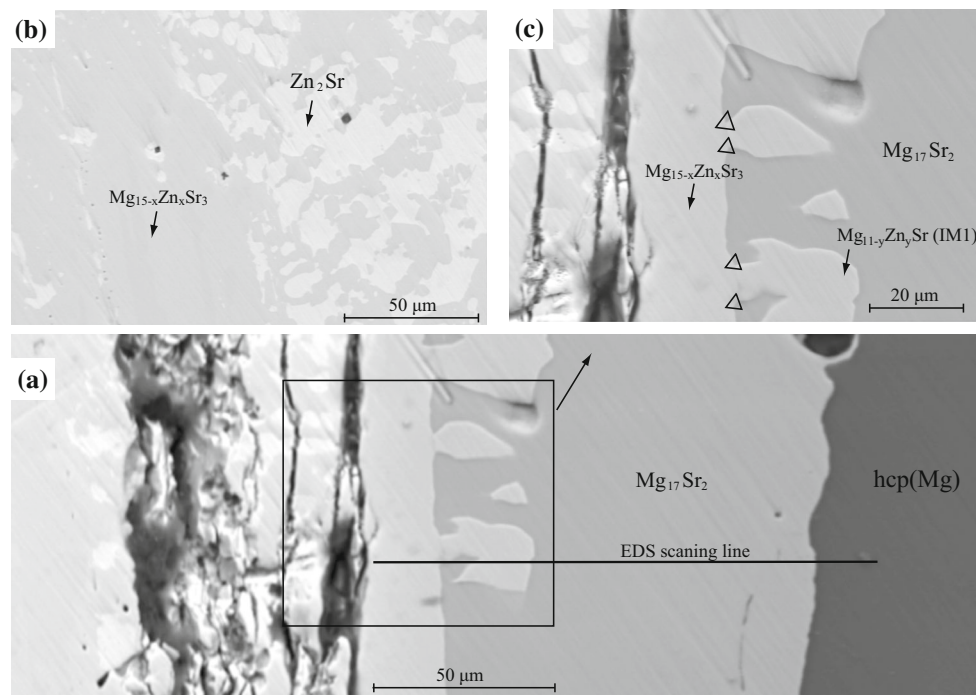
BSE images obtained from typical Mg–Zn–Sr ternary key samples are shown in Fig. 5a–i. The new ternary compound Mg_{11–y}Zn_ySr (4.7 < y < 9) observed in diffusion couples D1 and D2 was confirmed in the key samples

A8–A10, A12, and A15–A20 after annealing at 300 °C. In sample A10 (Mg₃Zn₈₇Sr₁₀), the three-phase equilibrium Zn₅Sr + Zn₁₃Sr + Mg_{11–y}Zn_ySr was observed as shown in Fig. 5a. According to the EPMA results of the constituted phase compositions in the key sample A10, the maximum solid solubility limit of Zn in the new phase Mg_{11–y}Zn_ySr was found to be 84.2 at%. A three-phase equilibrated microstructure MgZn₂ + Zn₁₃Sr + Mg_{11–y}Zn_ySr was observed in the sample A12 (Mg₁₆Zn₈₀Sr₄) as shown in Fig. 5b. A value close to the maximum solid solubility limit of Zn in phase Mg_{11–y}Zn_ySr was found to be 83.7 at% in sample A12. As shown in Fig. 5c, another three-phase equilibrium hcp (Mg) + Mg₁₇Sr₂ + Mg_{11–y}Zn_ySr was found in the key sample A19 (Mg₈₀Zn₁₅Sr₅). Deservedly, the minimum solid solubility limit of Zn in Mg_{11–y}Zn_ySr, in the Mg-rich region, was found to be 42.0 at% by EPMA.

The two-phase equilibrium Mg_{11–y}Zn_ySr + Mg_{15–x}Zn_xSr₃ was observed in the alloy sample A8 (Mg₃₅Zn₅₅Sr₁₀) as shown in Fig. 5d. This confirmed that Mg_{11–y}Zn_ySr is a single phase with a large solid solubility composition range of Zn without miscibility gap. The constituted phases in sample A8 were also confirmed using XRD as shown in Fig. 6a. Due to the complex crystal structure and atoms occupancy of Mg_{11–y}Zn_ySr, these XRD results will be discussed in a coming paper.

The solubility and equilibria of compound Mg_{15–x}Zn_xSr₃ were re-analyzed using samples A1–A8, A13, A15, and A20–A23 based on the results from our previous work [19]. In the three-phase equilibrium Mg_{15–x}Zn_xSr₃ + Mg₁₇Sr₂ + Mg₃₈Sr₉ observed in the key sample A1 (Mg₈₃Zn₁Sr₁₆) (as shown in Fig. 5e), the minimum solid

Fig. 4 **a** BSE image of diffusion couple D2 (Mg– $\text{Mg}_{25}\text{Zn}_{55}\text{Sr}_{20}$); **b** BSE image of end-member of $\text{Mg}_{25}\text{Zn}_{55}\text{Sr}_{20}$; **c** enlarged BSE image of the boxed area from the lower image of D2



solubility limit of Zn in the compound $\text{Mg}_{15-x}\text{Zn}_x\text{Sr}_3$ was found to be 1.3 at%. The phase constitutions of key sample A1 was also confirmed by the XRD results. The X-ray diffraction pattern obtained from sample A1 is depicted in Fig. 6b, where the XRD peaks of $\text{Mg}_{15-x}\text{Zn}_x\text{Sr}_3$, $\text{Mg}_{17}\text{Sr}_2$, and $\text{Mg}_{38}\text{Sr}_9$ can be observed clearly. A BSE image of sample A15 ($\text{Mg}_{20}\text{Zn}_{65}\text{Sr}_{15}$) is shown in Fig. 5f, where the three-phase equilibrium $\text{Mg}_{15-x}\text{Zn}_x\text{Sr}_3 + \text{Mg}_{11-y}\text{Zn}_y\text{Sr} + \text{Mg}_{20}\text{Zn}_{62}\text{Sr}_{18}$ can be seen. The maximum solid

solubility of Zn in $\text{Mg}_{15-x}\text{Zn}_x\text{Sr}_3$ is thus confirmed to be 58.8 at%. Moreover, a third compound with about 18 at% Sr, designated as IM5 ($\text{Mg}_{20}\text{Zn}_{62}\text{Sr}_{18}$) in our previous work [19], was confirmed in sample A15 (see Fig. 5f). This compound was also observed in samples A9, A14, and A21 in the three-phase equilibria $\text{Mg}_{20}\text{Zn}_{62}\text{Sr}_{18} + \text{Zn}_5\text{Sr} + \text{Mg}_{11-y}\text{Zn}_y\text{Sr}$, $\text{Mg}_{20}\text{Zn}_{62}\text{Sr}_{18} + \text{Zn}_2\text{Sr} + \text{Zn}_5\text{Sr}$, and $\text{Mg}_{20}\text{Zn}_{62}\text{Sr}_{18} + \text{Mg}_{15-x}\text{Zn}_x\text{Sr}_3 + \text{Zn}_2\text{Sr}$, respectively. The element composition of IM5 obtained using EPMA/

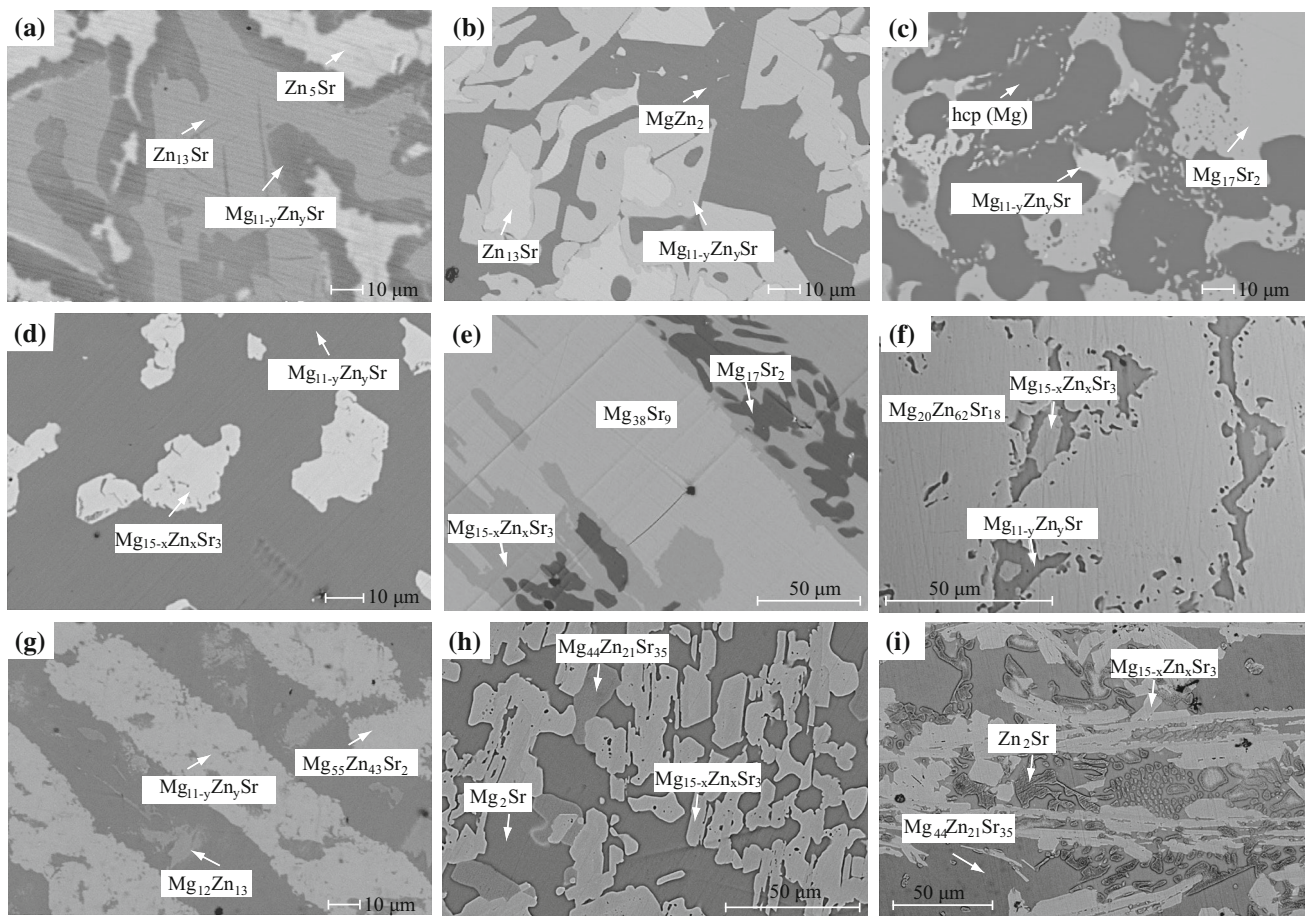


Fig. 5 Typical BSE images obtained from key samples annealed at 300 °C for 35 days: **a** A10 ($Mg_{33}Zn_{87}Sr_{10}$); **b** A12 ($Mg_{16}Zn_{80}Sr_4$); **c** A19 ($Mg_{80}Zn_{15}Sr_5$); **d** A8 ($Mg_{35}Zn_{55}Sr_{10}$); **e** A1 ($Mg_{83}Zn_7Sr_{16}$); **f** A15 ($Mg_{20}Zn_{65}Sr_{15}$); **g** A17 ($Mg_{49}Zn_{47}Sr_4$); **h** A23 ($Mg_{50}Zn_{25}Sr_{25}$); **i** A13 ($Mg_{25}Zn_{50}Sr_{25}$)

EDS tends to give a constant value of $Mg_{20}Zn_{62}Sr_{18}$; the formula “ $Mg_{20}Zn_{62}Sr_{18}$ ” was thus employed to designate IM5 in the present work. It is worth noting that more research work is needed to confirm the solid solubility and crystal structure of IM5 ($Mg_{20}Zn_{62}Sr_{18}$).

A fourth new compound, with a formula designated as “ $Mg_{55}Zn_{43}Sr_2$ (IM6)” based on its solid solubility composition range, was found in the alloy sample A17 ($Mg_{49}Zn_{47}Sr_4$), as shown in Fig. 5g, where the three-phase equilibrium $Mg_{55}Zn_{43}Sr_2 + Mg_{12}Zn_{13} + Mg_{11-y}Zn_ySr$ was observed. The solubility limit of Sr was measured to be about 2 at%, which is similar to the Ca content in the $Mg_{55}Zn_{43}Ca_2$ compound reported by Zhang et al. [20]. The compound $Mg_{55}Zn_{43}Sr_2$ was also observed in the sample A18 ($Mg_{60}Zn_{35}Sr_5$) in equilibrium with hcp (Mg) + $Mg_{11-y}Zn_ySr$ as listed in Table 3.

In the sample A23 ($Mg_{50}Zn_{25}Sr_{25}$), a fifth new compound, designated as IM2 in our previous work [19], was confirmed; it is in equilibrium with $Mg_2Sr + Mg_{15-x}$

Zn_xSr_3 (see Fig. 5h). This compound IM2 was also found in A13 ($Mg_{25}Zn_{50}Sr_{25}$) with the three-phase equilibrium $Zn_2Sr + IM2 + Mg_{15-x}Zn_xSr_3$ as shown in Fig. 5i. EDS/EPMA results show that the element composition in IM2 is close to the constant value of $Mg_{44}Zn_{21}Sr_{35}$. Consequently, the formula of IM2 was designated as “ $Mg_{44}Zn_{21}Sr_{35}$ ” in the present work.

The phase equilibria of the Mg–Zn–Sr ternary system in the composition range 0–35 at% Sr at 300 °C was obtained using alloy samples as shown in Fig. 7. Each of the determined three-phase equilibrium was labeled with different colors for easy reading purpose. All the compositions of the constituent phases of the equilibrated Mg–Zn–Sr ternary samples were determined by EPMA/EDS and are listed in the Table 3. Samples labelled with a star “*” were analyzed using EDS and corrected using EPMA standards. The phase constitutions and compositions of A1–A8 and A15 were reinvestigated based on the results

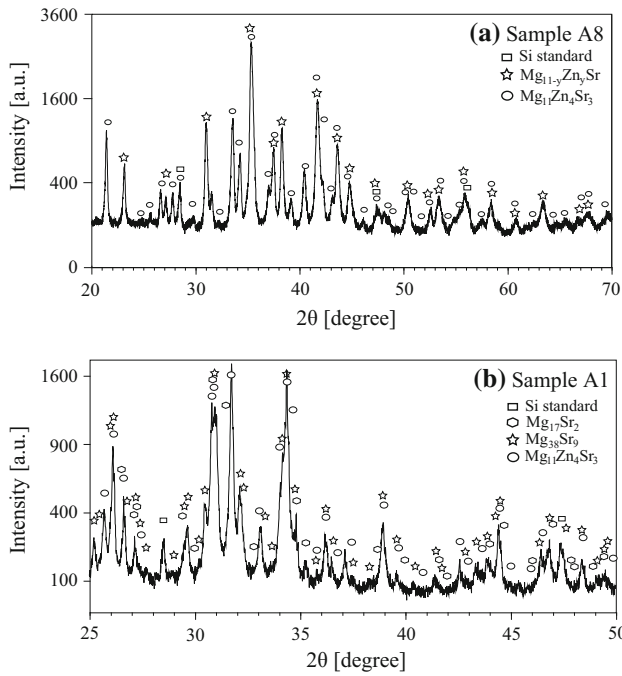
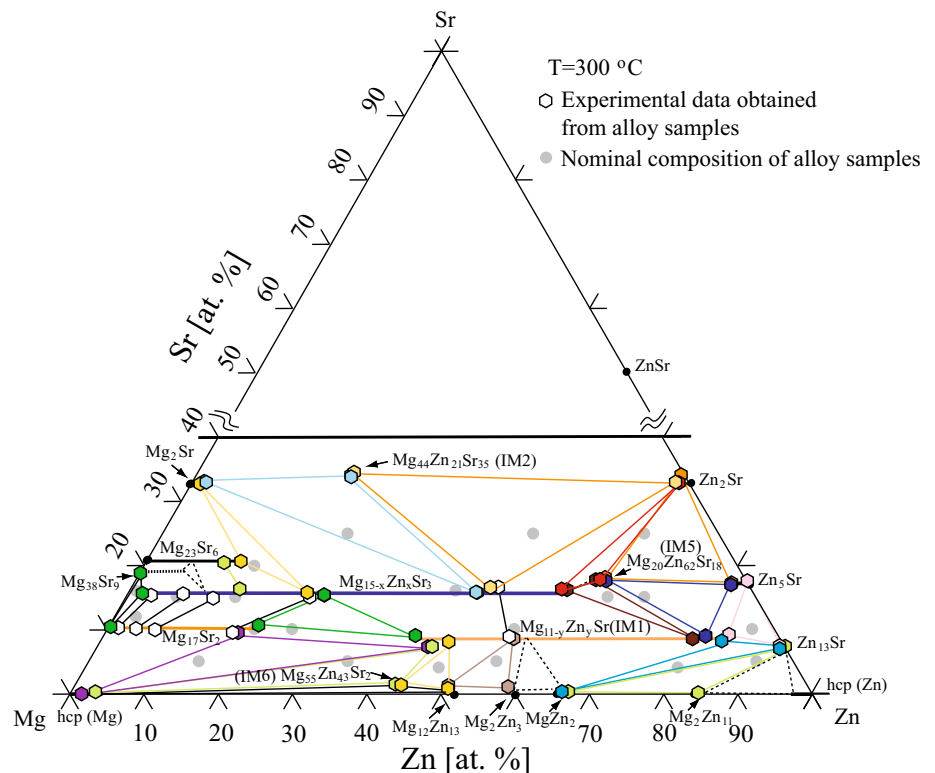


Fig. 6 X-ray diffraction patterns obtained from: **a** $\text{Mg}_{35}\text{Zn}_{55}\text{Sr}_{10}$ and **b** $\text{Mg}_{83}\text{Zn}_1\text{Sr}_{16}$ alloys annealed at 300 °C for 35 days

obtained in our previous work [19]. Both phase equilibria relationships and compositions, obtained using equilibrated alloys and diffusion couple techniques, are in good agreement.

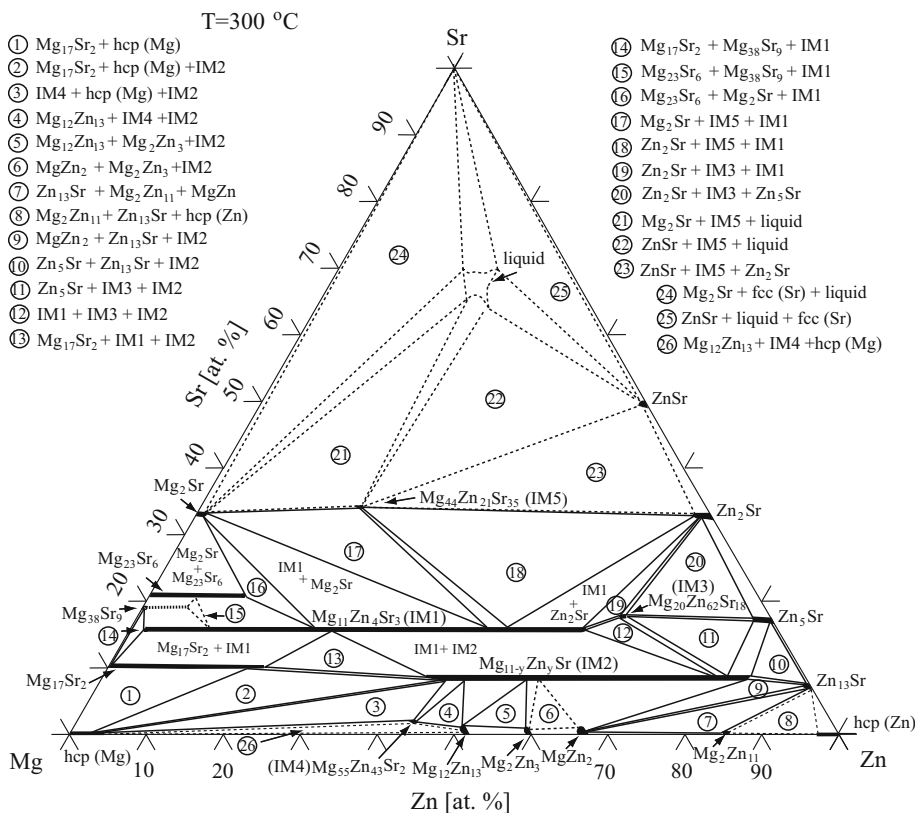
Fig. 7 Isothermal section of the Mg–Zn–Sr ternary system at 300 °C with experimental data obtained from key samples



Isothermal section

The isothermal section of the Mg–Zn–Sr ternary system at 300 °C, obtained using alloy samples and diffusion couples, is shown in Fig. 8. Sixteen three-phase domains, lying in the composition range 0–35 at% Sr, have been accurately determined in the present work. Four new ternary compounds, $\text{Mg}_{11-y}\text{Zn}_y\text{Sr}$ (IM, $4.7 < y < 9$), $\text{Mg}_{44}\text{Zn}_{21}\text{Sr}_{35}$ (IM2), $\text{Mg}_{20}\text{Zn}_{62}\text{Sr}_{18}$ (IM5), and $\text{Mg}_{55}\text{Zn}_{43}\text{Sr}_2$ (IM6) along with the previous reported compound $\text{Mg}_{15-x}\text{Zn}_x\text{Sr}_3$, were found in the present work. The solid solubility limits of Zn in $\text{Mg}_{15-x}\text{Zn}_x\text{Sr}_3$ ranges between 1.3 and 58.8 at% with a constant Sr content of 16.7 at% [19]. The solid solubility limits of Zn (substituting to Mg) in $\text{Mg}_{11-y}\text{Zn}_y\text{Sr}$ ranges between 42.0 and 84.2 at% at a nearly constant Sr content of about 8 at%. According to the present results obtained from alloy samples as listed in Table 3, the compounds $\text{Mg}_{44}\text{Zn}_{21}\text{Sr}_{35}$, $\text{Mg}_{20}\text{Zn}_{62}\text{Sr}_{18}$, and $\text{Mg}_{55}\text{Zn}_{43}\text{Sr}_2$ have limited solid solubility limits. They are treated as stoichiometric compounds by the present authors. The maximum solid solubility limits of Zn in $\text{Mg}_{17}\text{Sr}_2$ and $\text{Mg}_{23}\text{Sr}_6$ were measured to be 20.2 and 12.4 at% with Zn substitution by Mg at constant Sr contents of 10.7 and 20.0 at%, respectively. The solubility limits of Sr in the hcp (Mg), hcp (Zn), and Mg–Zn binary terminal compounds are inferior to 1.5 at%. The solid solubility limits of Mg in Zn_2Sr and Zn_5Sr were found to be about 1.8 and 2.6 at%,

Fig. 8 Isothermal section of the Mg–Zn–Sr ternary at 300 °C



respectively. The solubility limit of Mg in the Zn₁₃Sr compound is negligible (around 0.1 at%).

There are still four undetermined three-phase assemblages in the Mg–Zn rich region: Mg₃₈Sr₉ + Mg₂₃Sr₆ + Mg_{15–x}Zn_xSr₃, Mg₂Zn₃ + Mg_{11–y}Zn_ySr + MgZn₂, hcp (Zn) + Mg₂Zn₁₁ + Zn₁₃Sr, and hcp (Mg) + Mg₅₅Zn₄₃Sr₂ + Mg₁₂Zn₁₃. They are indicated with dashed lines in Fig. 8. Phase equilibria in the Sr-rich region (above 35 at%) were proposed as inferred by the authors based on the results reported for the Mg–Zn–Ca ternary system [20]. Further experiment will be necessary to verify them. Crystal structure analysis and thermal stability of the ternary compounds Mg_{11–y}Zn_ySr, Mg₄₄Zn₂₁Sr₃₅, Mg₂₀Zn₆₂Sr₁₈, and Mg₅₅Zn₄₃Sr₂ are still needed.

Conclusions

The isothermal section of the Mg–Zn–Sr ternary system at 300 °C, in the composition region 0–35 at% Sr, has been investigated using diffusion couples and key samples. The ternary compounds Mg_{11–y}Zn_ySr (IM1, 4.7 < y < 9), Mg₄₄Zn₂₁Sr₃₅ (IM2), Mg₂₀Zn₆₂Sr₁₈ (IM5), and Mg₅₅Zn₄₃Sr₂ (IM6) were found and their solid solubility limits were determined. Sixteen three-phase domains were determined. The extended solid solubility limits of all the binary

compounds, except ZnSr, were also determined in the Mg–Zn–Sr ternary system. The isothermal section of the Mg–Zn–Sr system at 300 °C was drawn. The remaining four three-phase domains in the Mg–Zn rich region were proposed as follows: Mg₃₈Sr₉ + Mg₂₃Sr₆ + Mg_{15–x}Zn_xSr₃, Mg₂Zn₃ + Mg_{11–y}Zn_ySr + MgZn₂, hcp (Zn) + Mg₂Zn₁₁ + Zn₁₃Sr, and hcp (Mg) + Mg₅₅Zn₄₃Sr₂ + Mg₁₂Zn₁₃. Phase equilibria in the Sr-rich region (above 35 at%) were proposed as inferred by the authors.

Acknowledgements Financial support from General Motors of Canada Ltd., and the Natural Sciences and Engineering Research Council of Canada through the CRD grant program is gratefully acknowledged. The support in the experimental part from Mr. Tian Wang, Mr. Xin Zhang, and Dr. Dmytro Kevorkov from Concordia University, and Mr. Lang Shi from McGill University is acknowledged by the authors.

Compliance with ethical standards

Conflict of interest The authors declare that they have no conflict of interest.

References

1. Polmear I (1994) Magnesium alloys and applications. Mater Sci Tech Lond 10(1):1–16

- Avedesian MM, Baker H (1999) ASM specialty handbook: magnesium and magnesium alloys, vol 274. ASM International
- Gao X, Nie J (2007) Characterization of strengthening precipitate phases in a Mg–Zn alloy. *Scripta Mater* 56(8):645–648
- Kainer KU, Kaiser F (2003) Magnesium alloys and technology. Wiley Online Library
- Aljarrah M, Medraj M (2008) Thermodynamic modelling of the Mg–Ca, Mg–Sr, Ca–Sr and Mg–Ca–Sr systems using the modified quasichemical model. *Calphad* 32(2):240–251
- Janz A, Schmid-Fetzer R (2009) Thermodynamics and constitution of Mg–Al–Ca–Sr–Mn alloys: part I. experimental investigation and thermodynamic modeling of subsystems Mg–Ca–Sr and Al–Ca–Sr. *J Phase Equilib Diff* 30(2):146–156
- Liu H, Chen Y, Zhao H, Wei S, Gao W (2010) Effects of strontium on microstructure and mechanical properties of as-cast Mg-5wt.% Sn alloy. *J Alloy Compd* 504(2):345–350
- Baril E, Labelle P, Pekguleryuz M (2003) Elevated temperature Mg–Al–Sr: creep resistance, mechanical properties, and microstructure. *J Min Met Mater Soci* 55(11):34–39
- Hirai K, Somekawa H, Takigawa Y, Higashi K (2005) Effects of Ca and Sr addition on mechanical properties of a cast AZ91 magnesium alloy at room and elevated temperature. *Mater Sci Eng A* 403(1):276–280
- Ghosh P, Mezbahul-Islam MD, Medraj M (2012) Critical assessment and thermodynamic modeling of Mg–Zn, Mg–Sn, Sn–Zn and Mg–Sn–Zn system. *Calphad* 36:28–43
- Meng F, Wang J, Liu L, Jin Z (2010) Thermodynamic modeling of the Mg–Sn–Zn ternary system. *J Alloy Compd* 508(2):570–581
- Wang J, Hudon P, Kevorkov D, Chartrand P, Jung I-H, Medraj M (2014) Experimental and thermodynamic study of the Mg–Sn–In–Zn quaternary system. *J Alloy Compd* 588:75–95
- Agarwal R, Fries SG, Lukas HL, Petzow G, Sommer F, Chart TG, Effenberg G (1992) The Mg–Zn system. *Z Metallkd* 83:216–223
- Nayeb-Hashemi A, Clark J (1986) The Mg–Sr (magnesium–strontium) system. *J Phase Equilib* 7(2):149–156
- Bruzzone G, Merlo F (1983) The Sr–Zn system. *J Less-common Met* 92(1):75–79
- Clark J, Rhines F (1957) Central region of the Mg–Zn phase diagram. *Trans Am Inst Min Metall Eng* 209:425–430
- Aljarrah M, Aghaulor U, Medraj M (2007) Thermodynamic assessment of the Mg–Zn–Sr system. *Intermetallics* 15(2):93–97
- Dinsdale AT (1991) SGTE data for pure elements. *Calphad* 15:317–425
- Wang J, Zhang Y-N, Hudon P, Jung I-H, Chartrand P, Medraj M (2015) Experimental study of the crystal structure of the Mg_{15–x}Zn_xSr₃ ternary solid solution in the Mg–Zn–Sr system at 300 °C. *J Mater Des* 86:305–315
- Zhang Y-N, Kevorkov D, Liu XD, Bridier F, Chartrand P, Medraj M (2012) Homogeneity range and crystal structure of the Ca₂Mg₅Zn₁₃ compound. *J Alloy Compd* 523:75–82
- Wang J, Jiajia H, Chartrand P, Jung I-H (2014) Thermodynamic optimizations on the binary Li–Sn system and ternary Mg–Sn–Li system. *Calphad* 47:100–113
- Wang J, Hudon P, Kevorkov D, Chartrand P, Jung I-H, Medraj M (2014) Experimental and thermodynamic study of the Mg–Sn–In–Zn quaternary system. *J Alloy Compd* 588:75–95
- Wang J, Miao N, Chartrand P, Jung I-H (2013) Thermodynamic evaluation and optimization of the (Na + X) binary systems (X = Ag, Ca, In, Sn, Zn) using combined Calphad and first-principles methods of calculation. *J Chem Thermodyn* 66:22–33
- Wang J, Hudon P, Kevorkov D, Chartrand P, Jung I-H, Medraj M (2014) Thermodynamic and experimental study of the Mg–Sn–Ag–In quaternary system. *J Phase Equilib Diff* 35(3):284–313
- Zhang Y-N, Kevorkov D, Bridier F, Medraj M (2011) Experimental study of the Ca–Mg–Zn system using diffusion couples and key alloys. *Sci Technol Adv Mater* 12(2):025003
- Zhang Y-N, Kevorkov D, Li J, Essadiqi E, Medraj M (2010) Determination of the solubility range and crystal structure of the Mg-rich ternary compound in the Ca–Mg–Zn system. *Intermetallics* 18(12):2404–2411
- Zhang Y-N, Rocher G, Briccoli B, Kevorkov D, Liu X, Altounian Z, Medraj M (2013) Crystallization characteristics of the Mg-rich metallic glasses in the Ca–Mg–Zn system. *J Alloys Compd* 552:88–97
- Wang J, Zhang Y-N, Hudon P, Jung I-H, Medraj M, Chartrand P (2015) Experimental study on the phase equilibria of Mg–Zn–Ag ternary system at 300°C. *J Alloys Compd* 639:593–601
- Wang J, Jung I-H, Chartrand P (2015) Thermodynamic modeling on Ag–(Ca, Li, Zn) and Ca–(In, Li) binary systems. *Calphad* 50:68–81
- Villars P, Cenzual K (2007) Pearson’s crystal data, crystal structure database for inorganic compounds. ASM International, Materials Park